

Characterizing entanglement in pulsed parametric down-conversion using chronocyclic Wigner functions

Benjamin Brecht and Christine Silberhorn

Integrated Quantum Optics, University of Paderborn, Paderborn, Germany

(Received 27 February 2013; published 8 May 2013)

Pulsed parametric down-conversion (PDC) processes generate photon pairs with a rich spectral-temporal structure, which offer an attractive potential for quantum information and communication applications. We investigate the four-dimensional chronocyclic Wigner function $W_{\text{PDC}}(\omega_s, \omega_i, \tau_s, \tau_i)$ of the PDC state, which naturally lends itself to the pulsed characteristics of these states. From this function we derive the conditioned time-bandwidth product of one of the pair photons, a quantity which not only is a valid measure of entanglement between the PDC photons but also allows us to highlight a remarkable link between the discrete- and continuous-variable descriptions of PDC. We numerically analyze PDC processes with different conditions to demonstrate the versatility of our approach, which is applicable to a large number of current PDC sources.

DOI: [10.1103/PhysRevA.87.053810](https://doi.org/10.1103/PhysRevA.87.053810)

PACS number(s): 42.65.Lm, 42.65.Re

I. INTRODUCTION

In today's quantum optical applications, parametric down-conversion (PDC) sources are a well-established tool for the generation of a large variety of quantum states. Their versatility covers the heralding of single photons, the creation of highly entangled photon-pair states, and the generation of bright single-mode as well as two-mode squeezed beams of light [1–4]. Pumping the PDC sources with spectrally broad ultrafast pump pulses further increases the repertoire of realizable quantum states, including the generation of genuine single-photon quantum pulses [5] and the creation of multimode quantum frequency combs [6,7].

Naturally, the experimental progress during recent years has been accompanied by elaborate theoretical considerations which aim for a complete understanding of the PDC process [8–13]. However, when it comes to the description of PDC output states, two at first glance disparate methods are still prevailing.

In continuous-variable quantum optics, quantum states are typically described by their Wigner function, and the analysis concentrates on evaluating the fluctuations of two conjugate phase-space quadratures. Nonclassical features are mostly associated with negative values of the Wigner function or with quadrature fluctuations smaller than those of a coherent state. In this respect, nondegenerate PDC states exhibit reduced joint fluctuations of the conjugate $(X_s + X_i)$ and $(Y_s - Y_i)$ quadratures and can thus overcome an apparent Heisenberg's uncertainty relation. This feature is known as two-mode squeezing and is an intuitive way for depicting the entanglement which is generated in a PDC process.

In contrast, in the context of discrete-variable systems research mainly focusses on the photon-pair picture, neglecting higher-order photon number contributions but taking into account modal characteristics. The spectral-temporal properties of PDC states are commonly described by their complex-valued joint spectral amplitude (JSA) function $f(\omega_s, \omega_i)$, from which also the entanglement between signal and idler can be retrieved. However, this description has one major drawback. Generally, the measurements used to determine the joint spectral distribution of a PDC state are phase-insensitive intensity measurements and thus do not yield the JSA but

the joint spectral intensity (JSI) function. Therefore, any information hidden in the phase term of the JSA gets lost during measurement. This can be deceptive when trying to generate decorrelated PDC states, which are highly valuable for the heralded generation of pure single photons [5,14,15]. By judging the purity of the heralded photon from spectral intensity measurements only, one possibly overestimates the performance of the heralded single-photon source.

In this paper we combine the advantages of both continuous-variable and discrete-variable systems into another approach towards describing the spectral-temporal behavior of PDC states. We utilize the chronocyclic Wigner function formalism which is well known in classical ultrafast optics, where it is routinely used to describe the spectral-temporal properties of pulses [16] and forms the basis of ultrafast pulse-characterization schemes [17]. Here we apply it to a PDC pumped by an ultrafast pulse. Note that this approach naturally lends itself to the pulsed characteristics of PDC sources, and since the Wigner function is real valued, all quantities are accessible by direct measurements of the respective time and frequency distributions. We present a compact analytic expression for the Wigner function which is valid for a large number of current PDC sources and introduce the concept of a conditioned time-bandwidth product (TBP). In classical optics, the TBP of a pulse is ultimately bounded from below by the Fourier limit. However, this paradigm does not hold true in the quantum regime. In particular we show that, for PDC states, spectral-temporal entanglement between signal and idler overcomes this classical boundary and the conditioned TBP forms a valid measure of entanglement.

II. DERIVATION OF THE CHRONOCYCLIC WIGNER FUNCTION

In order to derive an analytic expression for the chronocyclic PDC Wigner function $W_{\text{PDC}}(\omega_s, \omega_i, \tau_s, \tau_i)$, we start by assuming a PDC state $|\psi\rangle$ of the form

$$|\psi\rangle = B \int d\omega_s d\omega_i f(\omega_s, \omega_i) \hat{a}^\dagger(\omega_s) \hat{b}^\dagger(\omega_i) |00\rangle. \quad (1)$$

Here, the parameter B is an overall coupling constant, \hat{a}^\dagger and \hat{b}^\dagger are the standard signal and idler creation operators, and

the function $f(\omega_s, \omega_i)$ is the complex-valued JSA which fully characterizes the generated state [9]. Note that we neglect any higher-order photon number contributions of the PDC state, which is a good approximation in the limit of low pump powers, and that we restrict our analysis to one dimension in space, which is applicable in the case of wave-guided PDC.

The chronocyclic Wigner function can then be retrieved from the PDC density operator $\hat{\rho} = |\psi\rangle\langle\psi|$ by a two-dimensional Wigner transform

$$\begin{aligned} W(\omega_s, \omega_i, \tau_s, \tau_i) &= \frac{1}{(2\pi)^2} \int_{-\infty}^{\infty} d\omega' d\omega'' e^{i\omega' \tau_s + i\omega'' \tau_i} \\ &\times \left\langle \omega_s - \frac{\omega'}{2}, \omega_i - \frac{\omega''}{2} \left| \hat{\rho} \right| \omega_s + \frac{\omega'}{2}, \omega_i + \frac{\omega''}{2} \right\rangle. \end{aligned} \quad (2)$$

Since we aim to present a compact analytical expression for $W_{\text{PDC}}(\omega_s, \omega_i, \tau_s, \tau_i)$, we introduce two simplifications, which do not limit our general theory. All calculations can be performed numerically for cases in which our simplified model does not yield a satisfying description.

First, we express the JSA in terms of Gaussian functions, with the constituents $\alpha(\omega_s, \omega_i)$ called the pump envelope function and $\phi(\omega_s, \omega_i)$ called the phase-matching function, which reflect energy and momentum conservation of the PDC process, respectively.

$$\begin{aligned} f(\omega_s, \omega_i) &= \alpha(\omega_s, \omega_i) \phi(\omega_s, \omega_i) = \exp\left(-\frac{\Delta\omega^2}{2\sigma^2} - ia\Delta\omega^2\right) \\ &\times \exp\left[-\gamma\left(\frac{L}{2}\Delta k\right)^2\right] \exp\left(i\frac{L}{2}\Delta k\right). \end{aligned} \quad (3)$$

Here, we introduced the abbreviation $\Delta\omega = \omega_p^{(0)} - \omega_s - \omega_i$, which denotes the difference between the central pump frequency $\omega_p^{(0)}$ and signal and idler frequencies ω_s and ω_i . The spectral width of the pump pulse is given by σ , the length of the waveguide by L , and Λ denotes the periodic poling period, deployed to remove the phase mismatch $\Delta k = k_p(\omega_p) - k_s(\omega_s) - k_i(\omega_i) - \frac{2\pi}{\Lambda}$ between pump, signal, and idler. In contrast to the standard description of PDC, we explicitly take into account a temporal chirp of the pump pulse, characterized by the parameter a .

The approximation of the phase matching with a Gaussian can experimentally be achieved by applying an appropriate spatial chirp to the poling period Λ [18]. However, this simplification is a good approximation for PDC sources in general.

Second, we use a Taylor series expansion of the phase mismatch Δk up to first order around the perfectly phase matched central frequencies $\omega_p^{(0)}$, $\omega_s^{(0)}$, and $\omega_i^{(0)}$ and end up with [19]

$$\Delta k \approx (k_p^{(1)} - k_s^{(1)})\nu_s + (k_p^{(1)} - k_i^{(1)})\nu_i, \quad (4)$$

where $k_{p,s,i}^{(1)}$ are the inverse group velocities of the pump, signal, and idler, given by the ratio between group refractive indices $n_{p,s,i}^{(g)}$ and the speed of light. Note that we neglect second-order contributions here since the group-velocity dispersion of the crystal does not play a role in the PDC investigated here [20]. In Eq. (4), the variables $\nu_s = \omega_s^{(0)} - \omega_s$ and $\nu_i = \omega_i^{(0)} - \omega_i$

describe the frequency offsets of the signal and idler from their perfectly phase matched central frequencies. By rewriting the JSA as a function of the frequency offsets ν_s and ν_i we find

$$\begin{aligned} f(\nu_s, \nu_i) &= \exp\left[-\frac{(\nu_s + \nu_i)^2}{2\sigma^2} - \frac{\gamma L^2}{4c^2}(n_{ps}\nu_s + n_{pi}\nu_i)^2\right] \\ &\times \exp\left[-ia(\nu_s + \nu_i)^2 + i\frac{L}{2c}(n_{ps}\nu_s + n_{pi}\nu_i)\right], \end{aligned} \quad (5)$$

where we abbreviated $n_{ij} = n_i^{(g)} - n_j^{(g)}$ for $i, j = p, s, i$ and used $k(\omega) = \frac{n(\omega)\omega}{c}$, with c denoting the speed of light. After straightforward calculations employing Eq. (2) we derive a compact analytic expression for the four-dimensional chronocyclic PDC Wigner function:

$$\begin{aligned} W(\nu_s, \nu_i, \tau_s, \tau_i) &= \sqrt{\frac{2}{\gamma} \frac{|B|^2 c \sigma}{L \pi |n_{si}|}} e^{-1/2\gamma} \exp\left[-\frac{1}{\sigma^2}(\nu_s + \nu_i)^2\right. \\ &\quad \left.- \frac{\gamma L^2}{2c^2}(n_{ps}\nu_s + n_{pi}\nu_i)^2 - 4a^2\sigma^2(\nu_s + \nu_i)^2\right] \\ &\times \exp\left[-\frac{2c^2}{\gamma L^2 n_{si}^2}(\tau_s - \tau_i)^2 - \frac{\sigma^2}{n_{si}^2}(n_{pi}\tau_s - n_{ps}\tau_i)^2\right. \\ &\quad \left.+ \frac{2c}{\gamma L n_{si}}(\tau_s - \tau_i)\right] \exp\left[\frac{4a\sigma^2}{n_{si}}(\nu_s + \nu_i)(n_{pi}\tau_s - n_{ps}\tau_i)\right]. \end{aligned} \quad (6)$$

Note that a nonvanishing chirp of the pump pulse introduces spectral-temporal correlations between the two sibling photons generated in the PDC which cannot be observed by common measurements of the spectral intensity distribution.

From Eq. (6) we can directly deduce the limits of our second simplification. As soon as signal and idler photons have similar group velocities, n_{si} becomes very small, and Eq. (4) is not valid anymore because higher-order terms have to be taken into account in the Taylor series expansion of the wave vectors. Thus, the analytic expression is not valid for degenerate type-I PDC sources, where the signal and idler share the same polarization. Numerical calculations have to be applied then. For most other PDC sources based upon type-II and nondegenerate type-I processes, however, this analytic expression is valid and provides a practical approach for studying the biphoton state.

III. ENTANGLEMENT BETWEEN THE PDC PHOTONS

Having derived an analytic expression for the chronocyclic PDC Wigner function, we now deploy it to analyze the entanglement between the signal and idler photons created during the PDC process. We start by calculating single-photon Wigner functions (SPWF) from the PDC Wigner function. Note that detailed considerations on the SPWF have also been presented in [21] that investigate the single-photon purity of a heralded PDC photon under several experimental conditions.

Here, we concentrate on the striking similarity between the spectral-temporal description of PDC states, common in discrete-variable quantum optics, and the Wigner formulation, used in the field of continuous-variable quantum optics, by

introducing the notion of a conditioned SPWF. To highlight the close relationship between the two approaches we first recall two-mode squeezing and the cooperativity, two concepts associated with continuous- and discrete-variable approaches, respectively. Thereafter we introduce the notion of the conditioned TBP and point out its link to both representations.

A. Continuous-variable description

In the context of continuous-variable systems, PDC states are mostly understood by deploying a four-dimensional Wigner function $W(X_1, Y_1, X_2, Y_2)$, where $X_{1,2}$ and $Y_{1,2}$ are conjugate quadratures of the signal and idler, respectively. The amount of two-mode squeezing ζ , which is tantamount to the amount of entanglement between the PDC photons, can be determined when regarding joint fluctuations of the signal and idler as

$$\Delta^2(X_1 + X_2) = \Delta^2(Y_1 - Y_2) = \exp(-2|\zeta|) \leq 1. \quad (7)$$

Thus when fixing X_2 and Y_2 to distinct values $X_2^{(0)}$ and $Y_2^{(0)}$, $\Delta^2(X_1 + X_2^{(0)})\Delta^2(Y_1 - Y_2^{(0)})$ can overcome Heisenberg's uncertainty limit. The fact that two quadratures of the same field of a PDC state can apparently be defined with arbitrary precision, or at least below the Heisenberg limit [22], exemplifies the Einstein-Podolsky-Rosen (EPR) paradox [23] and has been demonstrated in [24].

B. Discrete-variable description

The typical representation of the same state becomes quite different when employing the discrete-variable description of PDC for biphoton states. In contrast to the previous definition, higher-photon-number contributions are normally neglected in this approach. Extracting information on the entanglement between signal and idler photons is typically accomplished by means of the Schmidt decomposition of the JSA function [25], where $f(\omega_s, \omega_i)$ is decomposed into two sets of orthonormal basis functions, such that

$$f(\omega_s, \omega_i) = \sum_n \lambda_n \phi(\omega_s) \theta(\omega_i) \quad (8)$$

and the Schmidt coefficients λ_n fulfill the condition $\sum_n \lambda_n^2 = 1$. This, in turn, allows us to determine the so-called cooperativity $K = \sum_n 1/\lambda_n^4$, a quantity representing an established measure of entanglement between the PDC photons. When the photons are uncorrelated, the JSA function is separable, and only one basis mode for the signal and idler remains. Consequently, the cooperativity then equals 1. With increasing entanglement between the signal and idler, the cooperativity increases and approaches infinity for perfectly correlated photon pairs.

C. Four-dimensional chronocyclic Wigner function

We can now find an intuitive connection between both two-mode squeezing and the cooperativity. To this end we consider, on the one hand, the unconditioned chronocyclic SPWF, which we obtain by ignoring any knowledge about one of the two photons. On the other hand, we calculate the conditioned chronocyclic SPWF by fixing the arrival time and

frequency offset of one photon. The two functions are then given by

$$W_s^{(\text{uncond})}(\nu_s, \tau_s) = \int d\nu_i d\tau_i W_{\text{PDC}}(\nu_s, \nu_i, \tau_s, \tau_i), \quad (9)$$

$$W_s^{(\text{cond})}(\nu_s, \tau_s) = W_{\text{PDC}}(\nu_s, \tau_s; \nu_i = \nu_i^{(0)}, \tau_i = \tau_i^{(0)}). \quad (10)$$

In either of the two cases, the SPWF is described by a two-dimensional Gaussian function in the (ν_s, τ_s) plane. Retrieving the TBP $\Delta\nu_s \Delta\tau_s$ from this function is a matter of simple geometric considerations, which are detailed in [26]. Here we focus on its significance for new insights on the underlying physics of the generated state.

Because time and frequency share a Fourier relationship, a given spectral width of a light pulse enforces a minimum duration due to $\Delta\nu \Delta\tau \geq \text{const}$, where the value of the constant depends on the pulse shape and the employed width parameter of the pulse. We chose our normalization such that the Fourier relationship can conveniently be written as $\Delta\nu \Delta\tau \geq 1$. The TBP measures the similarity of the light pulse to its idealized version and is thus a measure of pulse quality. It has been shown in [21] that for single-photon pulses a TBP which equals the lower bound is tantamount to a pure single-photon, whereas a larger TBP suggests impurity.

However, when employing entangled photon-pair states, we can also analyze the conditioned TBP of one of the pair photons. This expression can be retrieved from the conditioned SPWF presented in Eq. (10). By doing so a classically surprising and counterintuitive property emerges: the conditioned TBP can actually become smaller than 1, which is forbidden for classical light pulses. A similar phenomenon occurs in the case of two-mode squeezed states, where the joint fluctuations can overcome an apparent Heisenberg uncertainty relation, which is a fingerprint of the quantum feature of entanglement between the signal and idler.

For the upcoming analysis, we write down the analytical expression for the inverse conditioned TBP (ICTBP) that is $(\Delta\nu \Delta\tau)^{-1}$:

$$\delta_{\text{TBP}} = \sqrt{\frac{n_{\text{pi}}^2 + n_{\text{ps}}^2}{n_{\text{si}}^2} + \frac{\gamma L^2 \sigma^2 n_{\text{pi}}^2 n_{\text{ps}}^2}{2c^2 n_{\text{si}}^2} + \frac{2c^2(1 + 4a^2 \sigma^4)}{\gamma L^2 \sigma^2 n_{\text{si}}^2}}. \quad (11)$$

If the PDC photons are uncorrelated, the ICTBP δ_{TBP} equals 1. For increasing correlations between the signal and idler, the violation of the Fourier relationship becomes stronger, and the ICTBP increases.

IV. ANALYSIS OF THE CHRONOCYCLIC WIGNER FUNCTION

In this section, we evaluate the chronocyclic PDC Wigner function $W_{\text{PDC}}(\omega_s, \omega_i, \tau_s, \tau_i)$ for two distinct cases of PDC processes. First, we concentrate on the case of spectrally decorrelated PDC, which has received a lot of attention in recent years, as it allows for the direct heralding of pure single-photon pulses without the need for any filtering [5,14,15]. However, the implementation of these kinds of PDC sources still is a major experimental challenge, and in general, PDC processes exhibit strong spectral correlations between the signal and idler. Hence, we investigate, as a second case, a correlated PDC process.

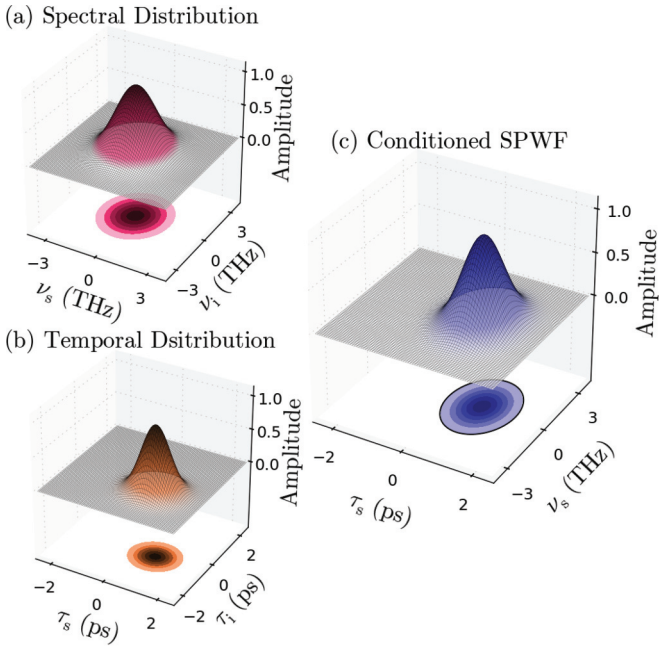


FIG. 1. (Color online) (a) JSI of the decorrelated PDC process. It is not possible to infer the signal frequency from measuring the idler frequency. (b) Corresponding JTI, exhibiting no correlations between signal and idler photon arrival times. (c) Conditioned SPWF of the signal photon. For further information see the text.

In the following we assume the PDC processes to be pumped by Fourier-limited pump pulses, which do not comprise any temporal chirp. Moreover, as a test-bed, we choose the PDC process first presented in [15]. It is realized in a potassium titanyl phosphate (KTP) waveguide pumped with ultrafast pump pulses around 775 nm and can generate decorrelated photons in orthogonal polarizations, centered around 1550 nm. By changing the spectral width of the pump pulses, the spectral-temporal correlations between signal and idler photons can smoothly be tuned.

A. Spectrally decorrelated PDC

In Figs. 1(a) and 1(b), we plot the JSI and joint temporal intensity (JTI) of the spectrally decorrelated PDC process, respectively. Obviously, no information on the signal can be gained from measuring the idler frequency offset or arrival time, meaning that signal and idler are generated in Fourier-limited pulses with flat phase distribution. Note that the offset of the JTI from the center of the figure reflects the different group velocities of the signal and idler in the nonlinear waveguide.

Figure 1(c) shows the conditioned SPWF, where we fixed the idler frequency offset and arrival time to zero. This choice is arbitrary and does not influence the shape of the conditioned SPWF, as long as the values are well inside the idler spectrum and duration. The black circle indicates the $1/e^2$ width of the unconditioned SPWF. Obviously, the conditioned and unconditioned SPWF are similar. In this case, the ICTBP equals 1, which corresponds to the signal photon residing in a Fourier-limited pulse. This result has been presented in [21], and it serves here as a cross-check for our approach.

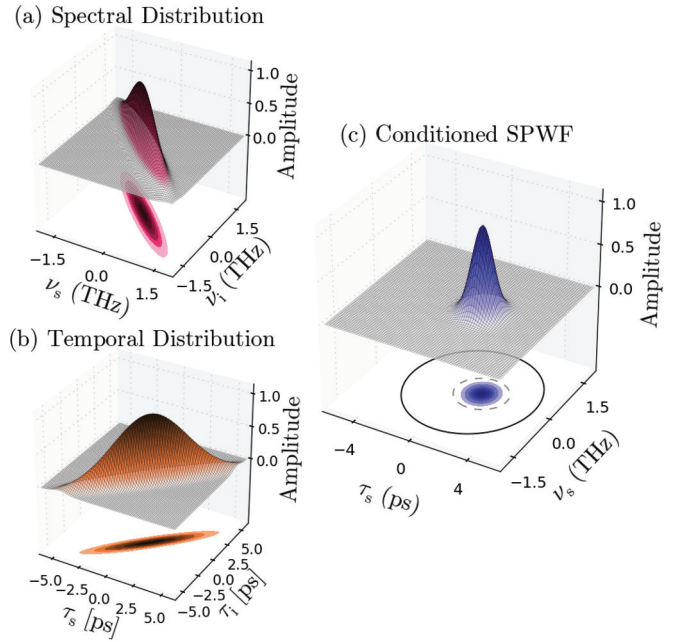


FIG. 2. (Color online) (a) JSI of the correlated PDC process. (b) Corresponding JTI, exhibiting inverted correlations. (c) Conditioned SPWF of the signal. For further information, see the text.

B. Spectrally correlated PDC

We now turn our attention to the more interesting and common case of a spectrally correlated PDC process, where we can infer the signal frequency from a measurement of the idler frequency.

In Figs. 2(a) and 2(b), we show the JSI and JTI of the spectrally correlated PDC, respectively. It can be easily seen that spectral anticorrelations correspond to temporal correlations, as expected for the two-dimensional Fourier transform between the two domains.

In Fig. 2(c) we plot the conditioned SPWF of the signal, where the black solid line indicates again the $1/e^2$ width of the unconditioned SPWF. In addition, the gray dashed line indicates the $1/e^2$ width of the SPWF of a pure single photon, which exhibits a TBP of 1. We can qualitatively deduce the TBP from the size of the SPWF and find that the TBP of the unconditioned signal is obviously larger than 1. Note that this corresponds to a mixed quantum state. In contrast, the TBP of the conditioned signal is smaller than 1, which is an indicator for the entanglement between the signal and idler.

V. ANALYSIS OF THE CONDITIONED TBP

In this section we deploy again the PDC process from [15] to actually calculate the ICTBP, as well as the cooperativity K . For the latter, we employ two approaches: on the one hand, we calculate K directly from the JSA given in Eq. (5); on the other hand, we calculate K from the JSI, which mimics the usual situation in the laboratory. The JSI is found by

$$F(\nu_s, \nu_i) = |f(\nu_s, \nu_i)|^2, \quad (12)$$

where we mention again that any phase information gets lost during this step. We concentrate on two scenarios. In the first case, we consider Fourier-limited pump pulses, whereas in the

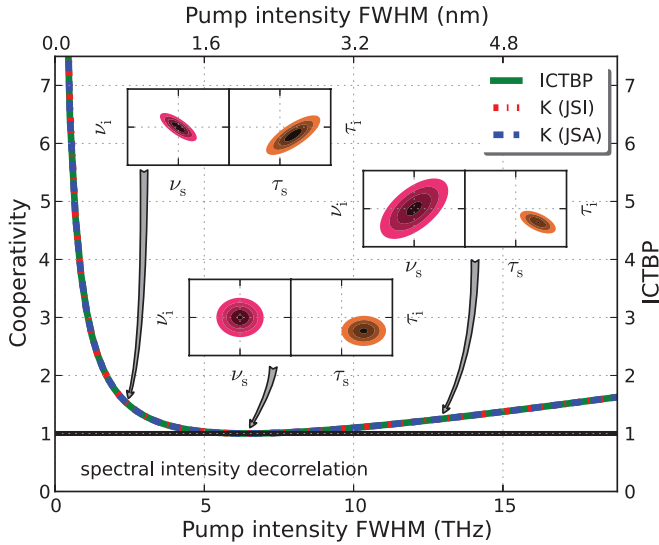


FIG. 3. (Color online) The ICTBP and the cooperativity K , calculated from the JSA and the JSI function for different degrees of spectral-temporal correlation between the signal and idler. The insets show the respective JSI (left) and JTI (right) for three distinct spectral widths of the pump pulses. For further information, see the text.

second case we turn our attention to the more realistic case of pump pulses, which exhibit a temporal chirp. To simulate different degrees of correlation between the signal and idler, we change the spectral width of the pump pulses σ . Note that the JSI becomes decorrelated for a pump pulse FWHM of around 2 nm.

In Fig. 3, we plot the ICTBP and the cooperativity K for the case of Fourier-limited pump pulses. The insets show the JSI (left) and JTI (right) for three different spectral widths of the pump. As expected, the cooperativities calculated from JSA and JSI are equal since in this situation no spectral-temporal correlations are encoded on the phase of the state. The ICTBP exactly equals the cooperativities, which justifies its proposed role as a measure of entanglement.

In the following, we investigate if the similarity between ICTBP and K persists when introducing a chirped pump and thus spectral-temporal correlations to the state. To this end, we consider a pump chirp of 3×10^5 fs² to clearly visualize its impact. Lower values of pump chirp decrease the investigated effects but do not completely suppress them.

In Fig. 4 we plot again the ICTBP and the cooperativity K . The insets show the JSI (left) and JTI (right) for the same spectral pump widths as in Fig. 3. Because of the spectral-temporal correlations, we now find strongly correlated signal and idler arrival times even for a decorrelated JSI. For the considered pump chirp, this also holds true for cases where we would usually expect an anticorrelated JTI, as depicted in the topmost inset. Since the pump chirp enters Eq. (5) in a quadratic phase term, we do not see its effect in intensity measurements. Therefore, the cooperativity calculated from the JSI strongly deviates from the one retrieved from the JSA. In contrast, the ICTBP again equals the phase-sensitive cooperativity from the JSA. Thus, full information on the entanglement between the signal and idler can be gained from

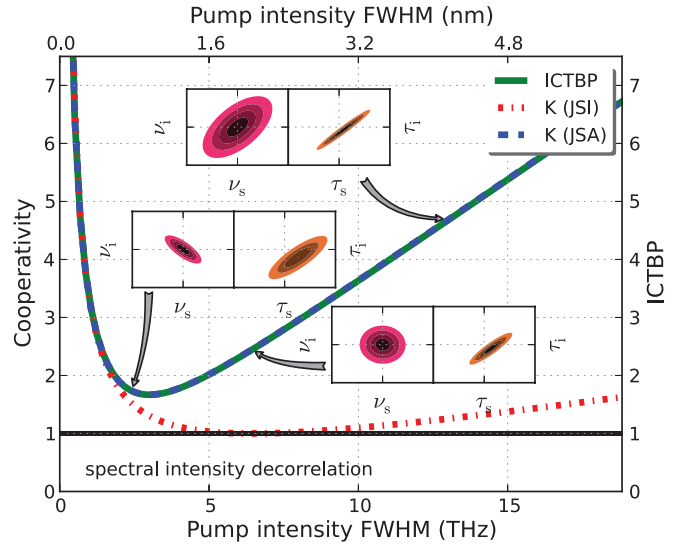


FIG. 4. (Color online) The ICTBP and the cooperativity K , calculated from the JSA and the JSI function for different degrees of spectral-temporal correlation between the signal and idler under the assumption of a chirped pump pulse. The insets show the respective JSI (left) and JTI (right) for three distinct spectral widths of the pump pulses. For further information, see the text.

the PDC Wigner function $W_{\text{PDC}}(\omega_s, \omega_i, \tau_s, \tau_i)$. As a practical note we point out that this knowledge can, in principle, be obtained from spectral and temporal intensity measurements but only if both JSI and JTI are measured.

Finally, we want to draw attention to the minimum in the ICTBP. In the case of Fourier-limited pump pulses depicted in Fig. 3, the minimum value of ICTBP of 1 is reached for spectral and temporal decorrelation of the signal and idler. However, as soon as the pump exhibits a temporal chirp, the position of the minimum moves towards stronger spectral anticorrelations, which partially compensate for the temporal correlations introduced by the chirp. In Fig. 4, the minimum of the ICTBP is at the point where the spectral anticorrelations are about as strong as the temporal correlations, as depicted in the leftmost inset.

VI. CONCLUSION

In this paper we have brought together well-known concepts from the discrete- and the continuous-variable descriptions of PDC to form an intuitive and complete description of the resulting state. We have derived a compact analytic expression for the four-dimensional chronocyclic Wigner function $W_{\text{PDC}}(\omega_s, \omega_i, \tau_s, \tau_i)$ of a PDC state, where we included the effects of different group velocities of the pump, signal, and idler fields and the effects of chirped pump pulses. In particular for the case of a pulsed pump this description naturally lends itself to the ultrafast characteristics of the generated signal and idler.

Utilizing this expression, we have introduced the ICTBP of one of the generated PDC fields. We have shown that this quantity exactly equals the cooperativity K , which can be obtained from the JSA of the PDC state and thus forms a valid measure of entanglement between the signal and idler. Moreover, we have shown that, given entanglement between

the signal and idler, the conditioned TBP becomes smaller than the classical Fourier limit. This surprising feature is similar to the phenomenon of two-mode squeezing in the continuous-variable description of PDC, where the conditioned quadrature fluctuations overcome an apparent Heisenberg's uncertainty limit and highlights the similarity between the two seemingly disparate descriptions of PDC.

We have analyzed the ICTBP for different degrees of correlation between the signal and idler and for situations with and without pump chirp, respectively. From the results, we could show that it is not sufficient to only measure the JSI or JTI of a PDC state to characterize the entanglement between

the signal and idler. One either has to measure both degrees of freedom or perform experimentally highly challenging, phase-sensitive measurements in time or frequency.

ACKNOWLEDGMENTS

The authors thank Andreas Christ and Georg Harder for fruitful discussions and helpful comments. The research leading to these results has received funding from the European Community's Seventh Framework Programme FP7/2001-2013 under Grant Agreement No. 248095 through the Integrated Project Q-ESSENCE.

-
- [1] P. G. Kwiat, K. Mattle, H. Weinfurter, A. Zeilinger, A. V. Sergienko, and Y. Shih, *Phys. Rev. Lett.* **75**, 4337 (1995).
 - [2] R. E. Slusher, P. Grangier, A. LaPorta, B. Yurke, and M. J. Potasek, *Phys. Rev. Lett.* **59**, 2566 (1987).
 - [3] M. E. Anderson, M. Beck, M. G. Raymer, and J. D. Bierlein, *Opt. Lett.* **20**, 620 (1995).
 - [4] Y. Zhang, H. Wang, X. Li, J. Jing, C. Xie, and K. Peng, *Phys. Rev. A* **62**, 023813 (2000).
 - [5] P. J. Mosley, J. S. Lundeen, B. J. Smith, P. Wasylczyk, A. B. U'Ren, C. Silberhorn, and I. A. Walmsley, *Phys. Rev. Lett.* **100**, 133601 (2008).
 - [6] G. J. de Valcárcel, G. Patera, N. Treps, and C. Fabre, *Phys. Rev. A* **74**, 061801 (2006).
 - [7] O. Pinel, P. Jian, R. M. de Araújo, J. Feng, B. Chalopin, C. Fabre, and N. Treps, *Phys. Rev. Lett.* **108**, 083601 (2012).
 - [8] C. M. Caves, C. Zhu, G. J. Milburn, and W. Schleich, *Phys. Rev. A* **43**, 3854 (1991).
 - [9] W. P. Grice and I. A. Walmsley, *Phys. Rev. A* **56**, 1627 (1997).
 - [10] A. B. U'Ren, C. Silberhorn, K. Banaszek, I. A. Walmsley, R. Erdmann, W. P. Grice, and M. G. Raymer, *Laser Phys.* **15**, 146 (2005).
 - [11] W. Wasilewski, A. I. Lvovsky, K. Banaszek, and C. Radzewicz, *Phys. Rev. A* **73**, 063819 (2006).
 - [12] Y. M. Mikhailova, P. A. Volkov, and M. V. Fedorov, *Phys. Rev. A* **78**, 062327 (2008).
 - [13] P. J. Mosley, A. Christ, A. Eckstein, and C. Silberhorn, *Phys. Rev. Lett.* **103**, 233901 (2009).
 - [14] X. Shi, A. Valencia, M. Hendrych, and J. P. Torres, *Opt. Lett.* **33**, 875 (2008).
 - [15] A. Eckstein, A. Christ, P. J. Mosley, and C. Silberhorn, *Phys. Rev. Lett.* **106**, 013603 (2011).
 - [16] J. Paye, *IEEE J. Quantum Electron.* **28**, 2262 (1992).
 - [17] C. Iaconis and I. A. Walmsley, *Opt. Lett.* **23**, 792 (1998).
 - [18] A. M. Brańczyk, A. Fedrizzi, T. M. Stace, T. C. Ralph, and A. G. White, *Opt. Express* **19**, 55 (2011).
 - [19] W. P. Grice, A. B. U'Ren, and I. A. Walmsley, *Phys. Rev. A* **64**, 063815 (2001).
 - [20] G. Brida, M. V. Chekhova, I. P. Degiovanni, M. Genovese, G. K. Kitaeva, A. Meda, and O. A. Shumilkina, *Phys. Rev. Lett.* **103**, 193602 (2009).
 - [21] X. Sanchez-Lozano, A. B. U'ren, and J. L. Lucio, *J. Opt. A* **14** (2011).
 - [22] M. D. Reid and P. D. Drummond, *Phys. Rev. Lett.* **60**, 2731 (1988).
 - [23] A. Einstein, B. Podolsky, and N. Rosen, *Phys. Rev.* **47**, 777 (1935).
 - [24] Z. Y. Ou, S. F. Pereira, H. J. Kimble, and K. C. Peng, *Phys. Rev. Lett.* **68**, 3663 (1992).
 - [25] C. K. Law, I. A. Walmsley, and J. H. Eberly, *Phys. Rev. Lett.* **84**, 5304 (2000).
 - [26] K. Laiho, K. N. Cassemiro, and C. Silberhorn, *Opt. Express* **17**, 22823 (2009).